Int. J. Electrochem. Sci., 10 **(2015)** 4044 - 4052

International Journal of
ELECTROCHEMICAL
SCIENCE
www.electrochemsci.org

Characterization of Spinel-type $LiCo_{0.04}Mn_{1.96}O_4$ Prepared by Liquid-phase Famless Combustion

Fangli Yang[1,2], *Jijun Huang*[1,2], *Jiabin Hao*[1,2], *Qiling Li*[1,2], *Hongli Bai*[1,2], *Changwei Su*[1,2], *Junming Guo*[1,2,*]

[1]Key Laboratory of Resource Clean Conversion in Ethnic Regions，Education Department of Yunnan, Yunnan Minzu University, Kunming 650500, PR China
[2] Key Laboratory of Chemistry in Ethnic Medicinal Resources, State Ethnic Affairs Commission & Ministry of Education, School of Chemistry and Biotechnology, Yunnan Minzu University, Kunming 650500, PR China
[*]E-mail: guojunming@tsinghua.org.cn

Received: 15 January 2015 / *Accepted:* 3 March 2015 / *Published:* 23 March 2015

In this paper, $LiCo_{0.04}Mn_{1.96}O_4$ cathode materials were prepared by a liquid-phase famless combustion synthesis at different temperatures and two-stage calcination. The single phase $LiCo_{0.04}Mn_{1.96}O_4$ was synthesised by liquid-phase famless combustion , the samples at 600℃and two-stage calcination have a better crystallinity. Two-stage calcination sample revealed the excellent electrochemical performance with an initial specific discharge capacity of 121.9 mAh g^{-1} at 0.2 C and a capacity retention of 80.6% after 60 cycles. The results showed that the electrochemical activity of $LiMn_2O_4$ can be improved by the increase of temperatures. The sample of two-stage calcination exhibited an excellent electrochemical activity.

Keywords: Lithium ion batteries; Cathode; Co doping; Liquid-phase famless combustion

1. INTRODUCTION

Lithium rechargeable batteries have become great appealing power source due to their high energy density, high power density, low cost and stable cycling lifepan [1]. Spinel $LiMn_2O_4$ are considered as the most promising materials for replacing $LiCoO_2$ as commercialization cathode material ascribed to its merits of low material cost, rich aboundance of Mn resource, low toxicity of Mn ion and environmental friendly. Recent surveys have shown that the preparation process is an important factor that affects the electrochemical performance of spinel $LiMn_2O_4$ cathode material. It is well known to all that traditional synthesis of $LiMn_2O_4$ mainly including: High temperature solid-state

process [2], sol–gel method [3], hydrothermal synthesis [4], co-precipitation method [5] and combustion method [6]. Spinel $LiMn_2O_4$ was firstly synthesized by the liquid-phase famless combustion which our team have detailed study [7]. Nevertheless, the capacity fading of $LiMn_2O_4$ is a fatal obstacle which limits its large-scale use. The reasons of fast decay capacity have been widely investigated and they were mainly divided into the following three aspects: (1) Jahn-Teller distortion [8-9], (2) the dissolution of Mn^{3+}into the electrolyte [10], (3) changes in crystallinity [11]. To overcome the aforementioned problems, many researchers have attempted to improve the structural stability and electrochemical performance of $LiMn_2O_4$ cathode material by ions doping and surface modified. However, for the ions doping, the doping ions should have a similar static energy ,valence state and ionic radius with Mn. In addition, The strength of M–O bonding is stronger than Mn–O bonding after ion doping , which can improve the structural stability. Studies showed that the common ions doping including Mg^{2+} [14], Cu^{2+}[15], Ni^{2+}[16], Al^{3+}[17], Co^{3+}[18]. Nowadays it is not ever reported the material $LiCo_{0.04}Mn_{1.96}O_4$ synthesized by the liquid-phase famless combustion.

In this work, to improve complex preparation process and capacity degradation of the spinel $LiMn_2O_4$, $LiCo_{0.04}Mn_{1.96}O_4$ cathode materials were synthesized by a liquid-phase fameless combustion at different temperatures and two-stage calcination. The influence of different calcination temperatures on the crystal structure and electrochemical properties of the $LiCo_{0.04}Mn_{1.96}O_4$ cathode materials were also investigated in detail to find the best way to improve the cycle prosperity of the $LiMn_2O_4$.

2. EXPERIMENTAL

2.1. Preparation of $LiCo_{0.04}Mn_{1.96}O_4$

$LiCo_{0.04}Mn_{1.96}O_4$ cathode materials prepared by a liquid-phase famless combustion [19]. First of all, lithium nitrate (AR, aladdin), manganese acetate (AR, aladdin) and cobalt acetate (AR, aladdin) were dissolved in 9 mol/L nitrate with a stoichiometric ratio of Li:Mn:Co=1:1.96:0.04. The solution was calcined at 400 ^{0}C, 500 ^{0}C and 600 ^{0}C for 3 h. The original $LiCo_{0.04}Mn_{1.96}O_4$ material was obtained (samples were marked I_{400}, I_{500} and I_{600}). And then the original $LiCo_{0.04}Mn_{1.96}O_4$ calcined 500 ^{0}C material was further calcined at 600 ^{0}C for 3 h, the two-stage calcined $LiCo_{0.04}Mn_{1.96}O_4$ was got (sample was marked II_{600}).

2.2 Characterization of $LiCo_{0.04}Mn_{1.96}O_4$ materials

The characterization of the $LiCo_{0.04}Mn_{1.96}O_4$ powders was characterized by X-ray diffraction (XRD, D/max-TTRIII, Japan) with Cu Kα radiation to identify the crystal structure and the measurement range was from 10° to 70°with 0.02° step size and scan speed was 4°min^{-1} at an operation current of 30 mA and voltage of 40 kV. Lattice parameters were obtained using Jade 5.0 software. The particle morphology of the $LiCo_{0.04}Mn_{1.96}O_4$ powders was observed by scanning electron microscopy (SEM, QUANTA-200 America FEI Company).

2.3. Electrochemical Studies of $LiCo_{0.04}Mn_{1.96}O_4$ Materials

The cathode was obtained of 80 wt% $LiCo_{0.04}Mn_{1.96}O_4$ powders (active materials), 10 wt% carbon black (conductive agent), and 10 wt% polyvinylidene fluoride (PVDF, binder) in N-methyl-2-pyrrolidone (NMP) solvent followed by coating onto Al foil current collector . The coated Al foil was punched to obtained 16 mm diameter. The prepared electrodes were dried at 120°C for overnight under vacuum. Using Celgard 2320-type membranes as the separator, the electrolyte was 1 mol L^{-1} $LiPF_6$ in EC/DMC(volume ratio 1:1) . The CR2025 coin-type cells with lithium foil as anode were assembled in a dry glove box filled with high purity argon gas. The galvanostatic charge and discharge tests of the cells were performed by Land electric test system CT200 (Wuhan Jinnuo Electronics Co, Ltd) at a current density of 0.2 C in the potential range between 3.20 V and 4.35 V. Cyclic voltammograms (CV) of the cells were measured at room temperature on a electrochemical workstation (IM6ex, ZAHNER-elektrik GmbH&Co. KG, Germany) in the voltage range from 3.6 to 4.5 V at the scann rate of 0.05 mV s^{-1}. EIS measurements were also conduct in two-electrode cells by using electrochemical workstation (IM6ex) with a frequency range from 0.1 to 100 KHz. All electrochemical measurements were performed at ambient temperature. The positive electrodes were adopted as the work electrode; the counter electrode and reference electrode were Li foil.

3. RESULTS AND DISCUSSION

3.1 X-ray diffraction analysis

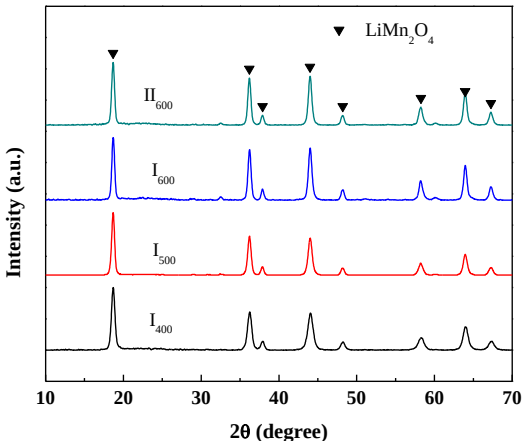

Figure 1. XRD patterns of $LiCo_{0.04}Mn_{1.96}O_4$ materials prepared at different calcination temperatures.

Fig.1 shows the X-ray diffraction patterns of $LiCo_{0.04}Mn_{1.96}O_4$ samples prepared by the liquid-phase famless combustion at 400 ^{0}C, 500 ^{0}C and 600 ^{0}C for 3 h and two-stage calcination at 600 ^{0}C for 3 h. All the characteristic diffraction peaks of spinel $LiMn_2O_4$ (JCPDS no. 35-0782) with the Fd3m space group [20] at the planes of (1 1 1), (3 1 1), (2 2 2), (4 0 0), (3 3 1), (5 1 1), (4 4 0) and (5 3 1), respectively. The XRD patterns demonstrate that the major spinel structure of $LiMn_2O_4$ is not seriously

changed after the Co doped. The particle size of the $LiCo_{0.04}Mn_{1.96}O_4$ samples can be calculated by Scherrer equation:

$$D = \frac{k\lambda}{(B\cos\theta)}$$

Where D is the average particle size, K is a constant, λ is the wavelength of the XRD. B is the broadening of the diffraction line measured at half maximum intensity and θ is the Bragg angle. Using scherrer equation, the lattice parameters calculated by Jade 5.0 shows in table. 1.

Table 1. The lattice parameters of $LiCo_{0.04}Mn_{1.96}O_4$ materials prepared at different calcination temperatures.

Sample	Lattice parameter
I_{400}	8.21934
I_{500}	8.22139
I_{600}	8.22622
II_{600}	8.22638

We can see that the lattice parameters increase with the increase of calcination temperature, which indicates that the enhancement of reaction temperature is beneficial for the expansion of unit cell [21]. In the cubic spinel $LiMn_2O_4$, Mn^{3+} and Mn^{4+} averagely occupy the octahedral 16d sites, Li^+ ion and O^{2-} locate at the tetrahedral 8a sites and 32e sites [22], respectively. Moreover, the radius of Co^{3+} ion (0.0630 nm) approaches that of Mn $^{3+}$ Ion (0.066 nm), which can be considered that Mn^{3+} is substituted Co^{3+} in the octahedral 16d sites. With the increase of the combustion temperatures, the diffraction peaks of $LiMn_2O_4$ are much stronger and the full width at half-maximum (FWHM) present narrower which indicate that appropriately increasing the reaction temperature can improve the crystallinity of the materials [23-24] and then increase the unit cell of $LiCo_{0.04}Mn_{1.96}O_4$.

3.2 Surface morphology

It can be observed from Fig. 2 that $LiCo_{0.04}Mn_{1.96}O_4$ materials prepared at 400 ^{0}C, 500 ^{0}C are exhibited an inhomogeneous distribution and serious agglomeration.

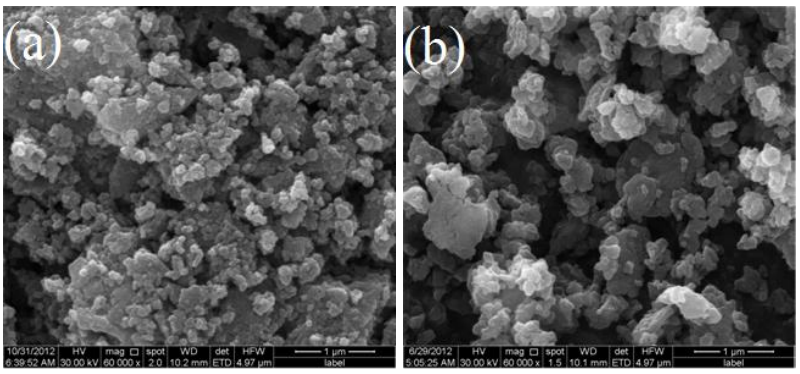

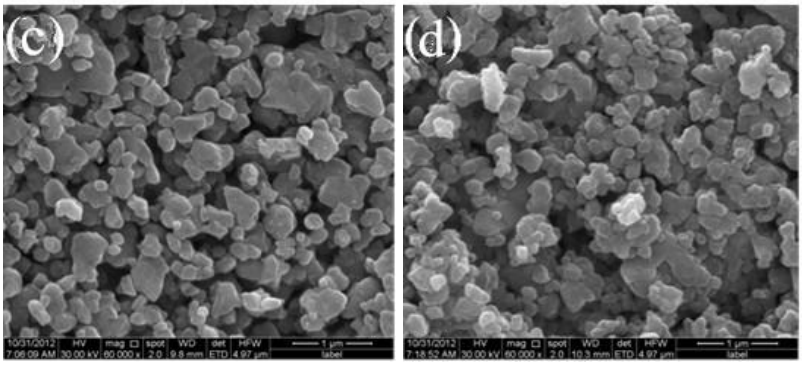

Figure 2. SEM of $LiCo_{0.04}Mn_{1.96}O_4$ materials prepared at different calcination temperatures (a:I_{400} b:I_{500} c:I_{600} d:II_{600}).

By contract, the SEM of the samples prepared at 600 ^{0}C and the two-stage calcination have an analogous spherical structure and clearer particle interface implying that the increase of calcination temperature can effectively promote the growth of grains, resulting in larger particle size and weaker agglomeration, which also consistent with the XRD.

3.3 Galvanostatic Cycling

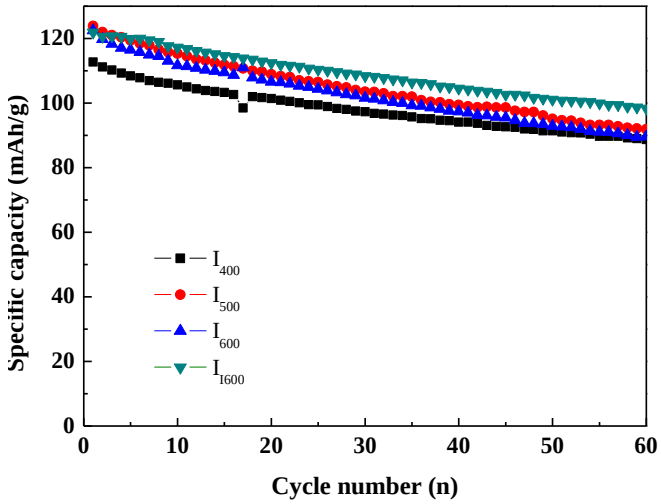

Figure 3. Cycling performances of $LiCo_{0.04}Mn_{1.96}O_4$ materials prepared at different calcination temperatures at 0.2 C rate.

Fig.3 presents the cycling performances of $LiCo_{0.04}Mn_{1.96}O_4$ samples prepared by the liquid-phase famless combustion at 400 ^{0}C, 500 ^{0}C and 600 ^{0}C for 3 h and two-stage calcination at 600^{0}C for 3 h. The cells cycled at 0.2 C in the voltage range of 3.20 V–4.35 V. The initial and 60th discharge capacity and capacity retention are summarized in Table. 2.

Table 2. Initial, 60th discharge capacities and capacity retention of $LiCo_{0.04}Mn_{1.96}O_4$ cathode materials.

Sample	discharge capacity (mA h g^{-1})		Capacity retention
	1st	60th	
I_{400}	112.7	88.7	78.7%
I_{500}	123.9	91.9	74.2%
I_{600}	122.5	89.6	73.1%
II_{600}	121.9	98.3	80.6%

It can be seen that the I_{400} sample delivers a lower initial capacity of 112.7 mA h g^{-1}. The II_{600} sample showed the highest capacity retention of 80.6% after 60 cycles at 0.2 C and its initial discharge specific capacity is 121.9 mA h g^{-1}. The results showed that discharge specific capacity and charging/discharging cycle efficiency of $LiMn_2O_4$ can be improved by two-stage calcination.

3.4 Cyclic voltammetry

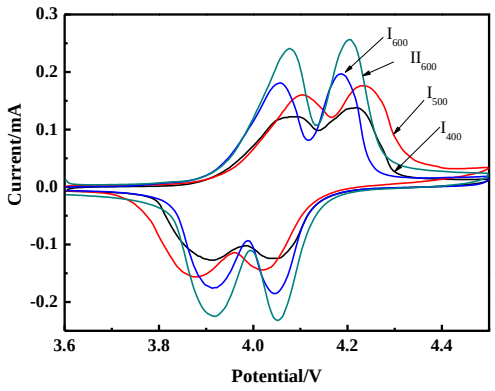

Figure 4. Cyclic voltammetry of $LiCo_{0.04}Mn_{1.96}O_4$ materials prepared at different calcination temperatures.

Fig. 4 shows the cyclic voltammetry of $LiCo_{0.04}Mn_{1.96}O_4$ samples prepared by the liquid-phase famless combustion at 400^0C, 500^0C and 600^0C for 3 h and two-stage calcination at 600^0C for 3 h. The cells cycled in the voltage range of 3.6 V– 4.5 V and at a scan rate of 0.05 mV s^{-1}. Two pairs of similar redox peaks locate at about 4.07 V/3.95 V and 4.20 V/4.10 V observed in the CV curves for all materials, which are corresponding to the two-stage intercalation/ deintercalation process of lithium in spinel $LiMn_2O_4$ [25-26]. The peak current and peak area of the I_{400} sample lower than other samples and its two redox peaks are even less distinguishable. With the increase of the calcination temperatures, the samples exhibit higher peak current and peak area. The II_{600} sample shows a higher peak and peak area, implying better electrochemical activity.

3.5. Electrochemical impedance spectroscopy

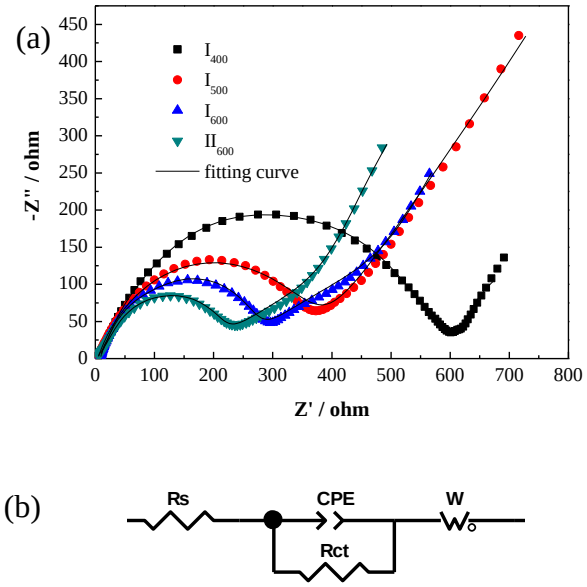

Figure 5. (a) Nyquist plots of the $LiCo_{0.04}Mn_{1.96}O_4$ products after the 10 rate cycles, (b) Equivalent circuit of EIS.

Fig. 5(a) presents the Nyquist plots of $LiCo_{0.04}Mn_{1.96}O_4$ samples prepared by the liquid-phase famless combustion at 400 ^{0}C, 500 ^{0}C and 600 ^{0}C for 3 h and two-stage calcination at 600 ^{0}C for 3 h after 10 charge–discharge cycles. The shapes of the Nyquist plots is similar, they are composed of a semicircle in the middle-high frequency (Hz) region and a straight line in the low frequency region. In the high frequency, an intercept value with the capacitive reactance at the Z real axis corresponding to the ohmic resistance of the electrolyte solution (R_s). The semicircle reflects the charge transfer resistance (R_{ct}). Constant phase element (CPE) represents a non-ideal capacitance of double layer. The straight line in the low frequency region represents Warburg impedance(W). The parameters of impedance spectra were simulated by Zview software. Fig. 5(b) shows the equivalent and the detailed fitting results shown in Table 3.

Table 3. The fitting values of electrochemical parameters obtained from EIS.

Sample	I_{400}	I_{500}	I_{600}	II_{600}
$R_s(\Omega)$	7.982	3.934	7.28	3.0
$R_{ct}(\Omega)$	579.4	361.8	260.9	199

It is observed that the cell impendence is mainly attributed to R_{ct}. The II_{600} sample shows a lowest R_{ct} (199 Ω), implying the lowest kinetic resistance for for lithium insertion and removal during electrochemical reaction which leads to a faster reaction rate of lithium ions in the charge/discharge

process [27]. Electrochemical impedance spectroscopy correspond with the other measurement, which further prove the II_{600} sample have an excellent electrochemical performance .

4. CONCLUSIONS

The main crystalline phase of all $LiCo_{0.04}Mn_{1.96}O_4$ materials prepared by the liquid-phase fameless combustion synthesis was the single spinel $LiMn_2O_4$. The crystallinity of the materials was improved with the increase of the temperatures and the II_{600} sample had the best crystallization. I_{400} and I_{500} samples were exhibited serious agglomeration but I_{600} and II_{600} showed an analogous spherical structure with average particle size 200-300nm . It was showed that 400℃sample had a lower initial discharge specific capacity of 112.7 mA h g^{-1}. But all the I_{500}, I_{600} and II_{600} materials revealed excellent electrochemical performance with initial discharge specific capacity exceed 120 mAh g^{-1} and the II_{600} material with a best capacity retention 80.6% after 60 cycles at 0.2 C. CV and EIS presented that the electrochemical activity can be increased by the temperatures and the II_{600} sample showed an excellent electrochemical activity .

ACKNOWLEDGEMENTS
This work was financially supported by the National Natural Science Foundation of China (51262031, 51462036), Program for Innovative Research Team (in Science and Technology) in University of Yunnan Province (2011UY09), Yunnan Provincial Innovation Team (2011HC008), the Natural Science Foundation of Yunnan Provincial Education Department (2014J079), and Innovation Program of Yunnan Minzu University (2013HXSRTY01, 2014YJZ10, 2014YJY74).

References

1. B. Xu, D. Qian, Z.Wang and Y. S. Meng, *Mater. Sci . Engineering: R: Reports*, *73*(2012)51-65.
2. Nukuda T, Inamasu T, Fujii A, *J. Power sources*, 146(2005) 611-616.
3. X. M. Liu, Z. D. Huang, Seiwoon, *J. Power Sources*, 195(2010) 4290-4296.
4. C. H. Jiang , S. X. Dou , H. K. Liu , *J. Power Sources*, 172(2007)410-415.
5. Thirunakaran R, Ravikumar R, Gopukumar S, *J. Alloys Comp*, 556(2013)266-273.
6. Riley L A, Van Atta S, Cavanagh A S, *J. Power Sources*, 196(2011)3317.
7. M. M. Chen, X. Y. Zhou, C. W. Su, M. W. Xiang and J. M. Guo, *Asian J. Chem*, 26(2014) 714-718
8. Yamada A, Tanaka M and Tanaka K, *J. Power sources*, 81(1999)73-78.
9. B. H. Deng, Nakamura. H, Yoshio. M, *Chem. Letters*, 32(2003)942-943.
10. Y. Xia , M. Yoshio, *J. Power sources*, 66(1997)129-133.
11. Y. Gao，J. R.Dahn, *Electrochem. Soc*, 143(1996)100-114.
12. Amatucci G G，Pereira N，Zheng T. *J. Power Sources*, 81(1999): 39-43.
13. Cho W，Ra W and Wakihara M, *J. Solid State Chem*, 176(2006)3534-3540.
14. M. W. Xiang, L. Q. Ye and C. C. Peng , *Ceram. Int*, 40(2014)10839-10845.
15. N Nakayama, I Yamada and Y. Huang, *Electrochim. Acta*, 54(2009)3428–3432.
16. Y. J. Wei , Kyung Wan Nam, Kwang Bum Kim and Gang Chen, *Solid State Ionics*, 177(2006)29–35.

17. Ki Woong Kim, Sun Woo Lee and Kyoo Seung Han, *Electrochim. Acta*, 48(2003)4223-4231.
18. Z. J. Wang, J. L. Du, Z. L.Li and Zhu Wu, *Ceram. Int*, 40 (2014) 3527–3531.
19. Y. Xia, M. Huang, J. M. Guo and Y. J. Zhang, *Advanced Materials Research*, 186 (2011) 7-10.
20. J. L. Wang, Z. H. Li, J. Yang, J. J. Tang, J. J. Yu, W.B. Nie, G.T. Lei and Q. Z. Xiao, *Electrochim. Acta*, 75 (2012) 115–122.
21. T. F. Yia, C. L. Haob, C. B. Yuea, R. S. Zhua and J. Shu, *Synthetic Metals*, 159 (2009) 1255–1260.
22. C.H. Jiang, S.X. Doub and H.K. Liu , *J. Power Sources*, 172 (2007) 410–415.
23. Manev V, Faulkner T and Engel J, *The First Hawaii Battery . Confer*, 1998: 228.
24. M Chen, S. J. Li and C Yang, *J. Univer Sci Technology Beijing*, *Mineral*, *Metallurgy*, *Material*, 15(2008)468-478.
25. Z H Li, J. Yang， J. L. Wang ， J. J. Tang， G. T. Lei and Q. Z. Xiao, *Microporous and Mesoporous Materials*, 162(2012)44-50.
26. Kuwabata S， Masui S and Yoneyama H. *Electrochim. Acta* , 44(1999)4593-4600.
27. B. Nageswara Rao, P. Muralidharan, P. Ramesh Kumar, M. Venkateswarlu and N. Satyanarayana, *Int. J. Electrochem. Sci*, 9 (2014) 1207 - 1220.